

УДК 535.37

Erko JALVISTE* and Aleksei TRESHCHALOV*

SPECTROSCOPIC STUDY OF JET-COOLED BENZOTRIAZOLE

(Presented by K. K. Rebane)

$S_1 \leftarrow S_0$ laser-induced fluorescence excitation spectrum (0—0 band at $34\,929\text{ cm}^{-1}$) and dispersed fluorescence spectra following the excitation into strong vibronic lines of benzotriazole, cooled in a supersonic jet, have been obtained. The rotational contours of different vibronic bands differ substantially. The crude structure of the dispersed fluorescence spectra is determined by a long progression (up to $v=6$) of $1\,410\text{ cm}^{-1}$ vibration in S_0 state (asymmetric stretching of the triazole part). It is supposed that different tautomers of benzotriazole correspond to S_0 and S_1 states.

1. Introduction

The use of supersonic molecular beams in preparing cold isolated gas-phase samples for spectroscopic study is a well-known technique nowadays. To our knowledge, from class of benzoderivates of five-membered heterocycles (BDFMH) only indole and its derivatives have been investigated thoroughly with a jet-cooling method because indole is the chromophore of amino-acid tryptophan. Information about indole, its derivatives and their complexes is derived from investigations of excitation- and dispersed fluorescence spectra [1], rotationally resolved band contours [2], torsional structure in the spectra of methyl-substituted indoles [3] and time-resolved fluorescence [4]. In addition, several nontraditional methods have been developed: rotational coherence spectroscopy by time-resolved fluorescence detection, which has given precise rotational constants for some tryptophan derivatives [5] and two-photon fluorescence excitation by linearly/circularly polarized light, which has enabled, for the first time, to identify the bands belonging to 1L_a state in the excitation spectrum of a jet-cooled indole [6].

UV absorption spectra are analysed for vapours of BDFMH molecules benzo(*b*)furan, indole, thianaphthene, indene [6], benzoxazole, benzimidazole, benzothiazole [7] and 2,1,3-benzothiadiazole [8]. For benzotriazole the identified IR and Raman spectra are available [9]. UV absorption, fluorescence, phosphorescence and polarization spectra of indole, indazole, benzimidazole and benzotriazole solutions have been presented in [10]. The spectroscopic study of jet-cooled benzotriazole, reported here, is aimed at obtaining information about the excited states of this molecule.

In principle, there can exist two planar tautomers (1H and 2H) of benzotriazole (Fig. 1) [11]. Unfortunately, no information about tautomers in the gas phase is available. A crystallographic study of solid benzotriazole [12] has revealed only 1H-tautomer. The problem is analogous in the case of 1,2,3-triazole molecule, where 2H-tautomers are the only species observed in the gas phase, while in solution both tautomers can be found [13].

* Institute of Physics, Estonian Academy of Sciences. 202400 Tartu, Riia 142, Estonia.

The near UV singlet-singlet transitions of BDFMH are $\pi^* \leftarrow \pi$ type transitions to two excited electronic states. 1L_a and 1L_b , allowed with in-plane transition dipole moment. For benzotriazole solution in cyclohexane the absorption band origins for 1L_a , 1L_b and 1B_b states are reported to be, respectively, at 34 200, 38 300 and 48 000 cm^{-1} [10]. These absorption bands are smooth without clearly visible vibrational structure.

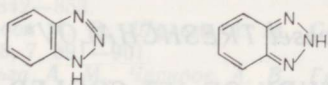


Fig. 1. Tautomers of benzotriazole: 1H-tautomer with C_s symmetry and 2H-tautomer with C_{2v} symmetry.

2. Experimental

Benzotriazole, twice recrystallized from ethanol, was heated in a nozzle chamber to 140 °C and seeded in 0.2 atm Ar gas, then the mixture was expanded into a vacuum through a 0.2 mm orifice. The vacuum of 10^{-3} Torr was maintained with a 700 l/s booster pump NVBM-0.5 backed by a 5 l/s rotary pump 2NVR-5D.

The fluorescence was excited with a frequency-doubled dye laser VL-18 (Rhodamine N and Rhodamine 6G dyes), pumped by ELI-73 excimer laser (typical repetition rate 5Hz). A frequency-doubled unfocused dye laser beam (FWHM 0.4 cm^{-1} , pulse energy 25 μJ , pulse to pulse stability 25%) crossed the jet at 5 mm downstream. The fluorescence excitation spectrum was obtained by measuring the total emission (with $f/1$ collection optics), the dispersed fluorescence spectra were measured with one half of a DFS-24 0.82 m double monochromator in the second grating order (with $f/3.6$ condenser). In both cases the signal was detected with a UV photomultiplier FEU-106, processed by a boxcar-integrator BCI-280 and recorded with a chart-recorder.

Although the resolution of VL-18 with an intracavity etalon was 0.1 cm^{-1} (in UV), the poor pulse-to-pulse stability limited the effective resolution of rotational band contours to 0.3 cm^{-1} . The dye laser and the monochromator were calibrated by using optogalvanic lines of iron/neon hollow cathode lamp. The amount of the scattered light was about 5% of the fluorescence intensity at excitation frequency when the strong bands were excited, therefore no scattering cut-off filter was used.

3. Results and discussion

Fig. 2 shows the $S_1 \leftarrow S_0$ fluorescence excitation spectrum (ES) of jet-cooled benzotriazole. The bands of the spectrum are tabulated in Table 1. The strongest 34929 cm^{-1} band in ES is assigned to an $S_1 \leftarrow S_0$ origin (0-0 band). For comparison, dispersed fluorescence (DF) spectrum of 0-0 band is presented in Fig. 3. The band frequencies of the spectrum relative to the laser frequency, the combination band assignments and the corresponding IR and Raman frequencies, with mode descriptions taken from [9], are summarized in Table 2.

All bands at the red side from 0-0 band are attributed to hot bands (started from some vibrationally excited ground state level), because their intensity relative to 0-0 band decreases when Ar pressure is raised. The increase of the relative intensity of hot bands is especially pronounced in the excitation spectrum of the stagnation temperature vapour obtained by attenuating the evacuation rate (ambient pressure 0.1 Torr).

The 34 365, 34 390, 34 808, 34 838, 34 929, and 35 409 cm^{-1} bands have hot satellites shifted to the red by about 90 cm^{-1} . If these satellites are caused by 90 cm^{-1} ground-state vibration, then corresponding band must appear in DF spectra. However, in the DF spectrum (Fig. 3) there is no band red-shifted by 90 cm^{-1} from the laser frequency — therefore, the six bands mentioned do not have the same excited state as their satellites have.

The 34 929 (0—0), 35 367 and 35 409 cm^{-1} bands have about 560 cm^{-1} red-shifted repetitions: 34 365, 34 808 and 34 847 cm^{-1} hot bands, respectively. This indicates that these hot bands start from 560 cm^{-1} vibrational level of S_0 state. Similar mode frequency appears in the Raman (570 cm^{-1}) and IR (562 cm^{-1}) spectra [9]. However, in the DF spectrum of 0—0 band there appears only one transition to 538 cm^{-1} ground state vibration, although in ES there exist two strong hot bands (34 365 and 34 390 cm^{-1}) whose distances from 0—0 band are 564 and 539 cm^{-1} .

The rapid intensity decrease in the ES above 36 100 cm^{-1} (1 170 cm^{-1} from the 0—0 band), where only weak 36 210 cm^{-1} band appears, can be attributed to the increase of the share of nonradiative processes: crossing to a dissociative state, like in the case of indole derivatives [4] or an inter-system crossing to some triplet states or an internal conversion into S_0 state. In addition, we can speculate that similar to photoisomerization of

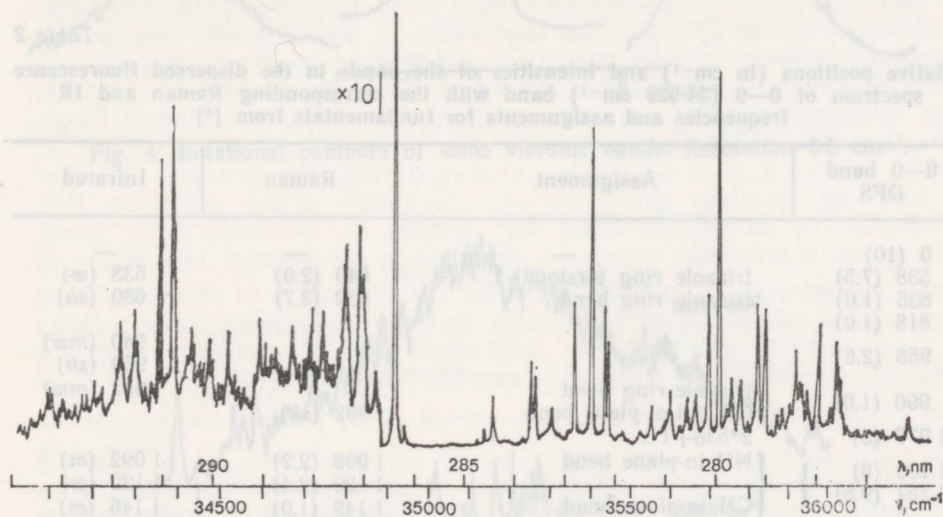


Fig. 2. Fluorescence excitation spectrum of jet-cooled benzotriazole. Band intensities are not normalized to the laser intensity.

Table 1

Vibronic band frequencies (cm^{-1}) and intensities in the fluorescence excitation spectrum. Absolute accuracy $\pm 2 \text{ cm}^{-1}$

34 272 (<i>vw</i>)	34 847 (<i>w</i>)	35 438 (<i>s</i>)	35 783 (<i>m</i>)
34 302 (<i>vw</i>)	34 929 (<i>vs</i>)	35 448 (<i>s</i>)	35 822 (<i>s</i>)
34 365 (<i>w</i>)	35 167 (<i>w</i>)	35 603 (<i>w</i>)	35 844 (<i>s</i>)
34 390 (<i>w</i>)	35 257 (<i>m</i>)	35 648 (<i>w</i>)	35 911 (<i>m</i>)
34 721 (<i>vw</i>)	35 266 (<i>m</i>)	35 672 (<i>w</i>)	35 970 (<i>s</i>)
34 749 (<i>vw</i>)	35 315 (<i>w</i>)	35 701 (<i>s</i>)	36 024 (<i>m</i>)
34 808 (<i>w</i>)	33 367 (<i>s</i>)	35 724 (<i>vs</i>)	36 210 (<i>w</i>)
34 838 (<i>w</i>)	35 409 (<i>vs</i>)	35 759 (<i>m</i>)	

styrene [14], if the excited state vibrational energy is comparable to the height of the potential barrier between the minima corresponding to the two tautomers (Fig. 1), a tautomerization occurs in S_1 state, which includes new channels for nonradiative processes.

It still remains unclear, if the observed S_1 state is to be assigned to 1L_a or 1L_b .

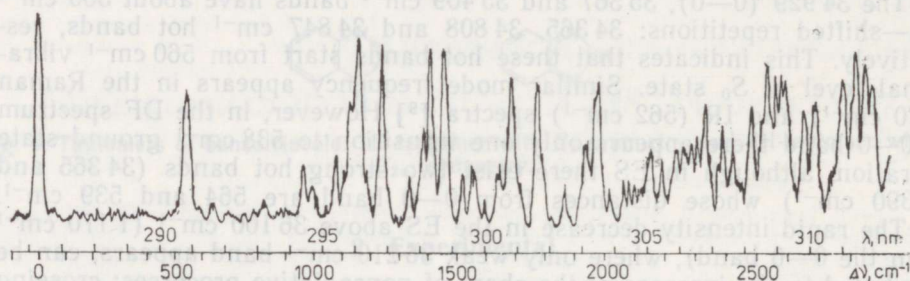


Fig. 3. Dispersed fluorescence spectrum following the excitation into 0-0 band at $34\,929\text{ cm}^{-1}$. Resolution 0.23 nm (26 cm^{-1}).

Table 2

Relative positions (in cm^{-1}) and intensities of the bands in the dispersed fluorescence spectrum of 0-0 ($34\,929\text{ cm}^{-1}$) band with the corresponding Raman and IR frequencies and assignments for fundamentals from [9]

0-0 band DFS	Assignment	Raman	Infrared
0 (10)	—	—	—
538 (7.5)	triazole ring torsion	540 (2.0)	533 (<i>w</i>)
635 (1.0)	triazole ring bend	632 (3.7)	630 (<i>sh</i>)
818 (1.0)			940 (<i>mw</i>)
956 (2.5)			950 (<i>sh</i>)
990 (1.0)	{ triazole ring bend CH out-of-plane bend	992 (<i>sh</i>)	982 (<i>mw</i>)
1 077 (3)	$2 \cdot 538 + 1$		
1 132 (6)	{ NH in-plane bend	1 098 (2.2)	1 092 (<i>m</i>)
1 157 (9.5)	{ CH in-plane bend	1 129 (2.4)	1 122 (<i>w</i>)
1 234 (9)	{ triazole ring breath (ν_s NNN)	1 149 (1.0)	1 146 (<i>m</i>)
1 335 (2.5)	{ CH in-plane bend	1 211 (2.7)	1 210 (<i>vs</i>)
1 382 (4.5)	{ benzene ring stretch	1 373 (5.3)	
1 410 (9)	{ triazole ring stretch	1 387 (9.3)	1 383 (<i>m</i>)
1 453 (9)	triazole ring stretch (ν_a NNN)		1 420 (<i>m</i>)
1 517 (2.5)	benzene ring stretch	1 458 (0.6)	1 458 (<i>m</i>)
1 552 (3)	$538 + 956 + 23$		
1 630 (4)	$538 + 990 + 24$		
1 685 (7)	$538 + 1\,077 + 15$		
1 702 (4)	$538 + 1\,132 + 15$		
1 776 (7)	$538 + 1\,157 + 7$		
1 870 (2)	$538 + 1\,234 + 4$		
1 939 (4.5)	$538 + 1\,335 - 3$		
1 975 (7.5)	{ $538 + 1\,382 + 19$	2 590 (7)	1 410 + 1 157 + 23
2 153 (3.5)	{ $538 + 1\,410 - 9$	2 645 (5.5)	1 410 + 1 234 + 1
2 332 (5.5)	$538 + 1\,453 + 16$	2 689 (7.5)	1 410 + 1 237 + 42
2 388 (5)			{ 1 410 + 1 335 + 25
2 421 (4)			1 410 + 1 382 - 22
	$1\,410 + 956 + 22$	2 770 (7)	2 813 (8)
	$1\,410 + 990 + 21$	2 813 (8)	$2 \times 1\,410 - 7$
		2 856 (9.5)	1 410 + 1 453 - 7

The rotational contours of some prominent bands in ES are shown in Fig. 4. The contours of 34 929 (0—0), 35 438 cm^{-1} bands and 34 365, 34 390 cm^{-1} hot bands are quite similar, but the contours of other bands differ drastically. Such difference is caused by the dependence of rotational constants (molecule geometry) or the direction of the transition

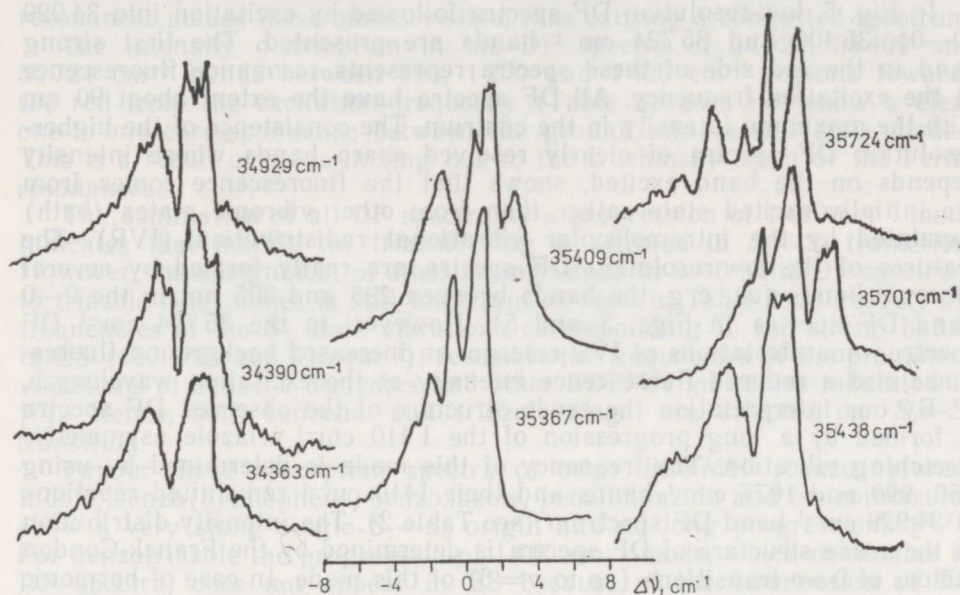


Fig. 4. Rotational contours of some vibronic bands. Resolution 0.3 cm^{-1} .

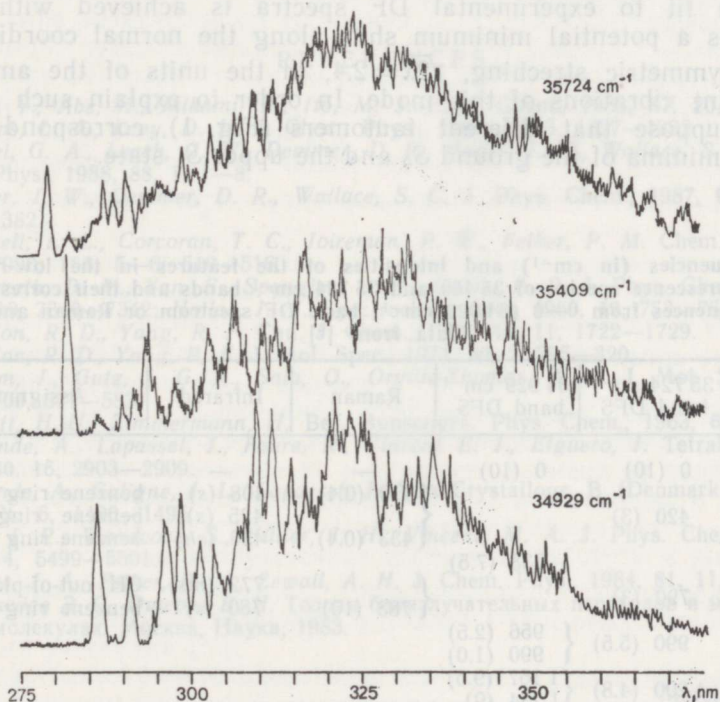


Fig. 5. Dispersed fluorescence spectra from the excitation of 34 929 (0—0), 35 409 and 35 724 cm^{-1} bands. Resolution 1 nm (115 cm^{-1}).

dipole moment on the vibronic band excited. Both effects can be explained with Hertzberg-Teller vibronic coupling to some upper state(s) allowed by transition(s) with different dipole moment direction. However, the geometrical configuration can be affected also by a strongly unharmonic vibration. The unharmonic potential may be connected with tautomerization in S_1 state.

In Fig. 5, low-resolution DF spectra followed by excitation into 34 929 (0—0), 35 409 and 35 724 cm^{-1} bands are presented. The first strong band in the red side of these spectra represents resonance fluorescence at the excitation frequency. All DF spectra have the extent about 90 nm with the maximum intensity in the centrum. The consistence of the higher-resolution DF spectra of clearly resolved sharp bands whose intensity depends on the band excited, shows that the fluorescence comes from the initially excited state rather than from other vibronic states (bath) populated by the intramolecular vibrational redistribution (IVR). The features of the low-resolution DF spectra are really formed by several vibronic bands (cf., e.g. the bands between 295 and 305 nm in the 0—0 band DF spectra in Figs. 3 and 5). However, in the 35 724 cm^{-1} DF spectrum manifestations of IVR emerge: an increased background fluorescence and a reduced fluorescence intensity at the excitation wavelength.

By our interpretation the crude structure of the observed DF spectra is formed by a long progression of the 1410 cm^{-1} triazole asymmetric stretching vibration. The frequency of this mode is determined by using 956, 990 and 1077 cm^{-1} bands and their 1410 cm^{-1} red-shifted repetitions in 34 929 cm^{-1} band DF spectrum (see Table 2). The intensity distribution in the crude structure of DF spectra is determined by the Franck-Condon factors of $0 \rightarrow v$ transitions (up to $v=6$) of this mode. In case of harmonic upper and ground state potentials with nearly equal vibrational frequencies the Franck-Condon factors for $0 \rightarrow v$ transitions are proportional to $x^v/v!$, where x is a parameter characterizing the distance between the potentials minima along normal coordinate of the vibration [15]. Reasonable fit to experimental DF spectra is achieved with $x=3$, which gives a potential minimum shift along the normal coordinate of triazole asymmetric stretching, $\sqrt{2x}=2.4$, in the units of the amplitude of zero point vibrations of this mode. In order to explain such a large shift we suppose that different tautomers (Fig. 1) correspond to the potentials' minima of the ground S_0 and the upper S_1 state.

Table 3

Relative frequencies (in cm^{-1}) and intensities of the features in the low-resolution dispersed fluorescence spectra of 35 409 and 35 724 cm^{-1} bands and their correspondence with frequencies from 0—0 (34 929 cm^{-1}) band DF spectrum or Raman and IR data from [9]

35 409 cm^{-1} band DFS	35 724 cm^{-1} band DFS	34 929 cm^{-1} band DFS	Raman	Infrared	Assignment
0 (10)	0 (10)	0 (10)	—	—	
	420 (3)		$\left\{ \begin{array}{l} 410 (0.4) \\ 433 (0.4) \end{array} \right.$	408 (s)	benzene ring bend
				425 (s)	benzene ring torsion
550 (1.5)		538 (7.5)		430 (sh)	benzene ring bend
	790 (3)		$\left\{ \begin{array}{l} 783 (10) \end{array} \right.$	772 (ms)	CH out-of-plane bend
				780 (s)	benzene ring breath
980 (2)	990 (5.5)	$\left\{ \begin{array}{l} 956 (2.5) \\ 990 (1.0) \end{array} \right.$			
1 210 (2.5)	1 200 (4.8)	$\left\{ \begin{array}{l} 1 157 (9.5) \\ 1 234 (9) \end{array} \right.$			
1 420 (6.5)	1 420 (5.5)	$\left\{ \begin{array}{l} 1 410 (9) \\ 1 453 (9) \end{array} \right.$			

The congestion of the bands, increasing to the red from the excitation frequency in DF spectra is explained by the increase of the density of S_0 vibrational states with the growth of the vibrational energy. More Fermi-resonances occur between the Franck-Condon allowed vibrations and «dark» combination modes if the density of these modes increases. The intensity redistribution to the combination modes due to the Fermi-resonances makes these modes visible, thus causing a congested spectrum.

The intensity distribution in the DF spectra of 34 929, 35 409 and 35 724 cm^{-1} bands between 990, 1 200 and 1 420 cm^{-1} regions towards the red from the excitation frequency (Table 3) does not show a clear one-to-one correspondence between the ground and excited state modes. This is a result of mode mixing due to the Dushinsky effect or the Fermi resonances.

The domination of all DF spectra by a progression of 1 410 cm^{-1} mode indicates that mainly the triazole ring is affected in $S_1 \leftarrow S_0$ transition. However, the assignment of other strong bands in 0-0 band DF spectrum to triazole ring modes is still uncertain as seen in Table 2. Moreover, the frequencies of the S_1 state vibrations corresponding to the strong bands in ES (480, 795 and 915 cm^{-1}), resemble the frequencies of the prominent vibrations of benzene derivatives and other BDFMH molecules tabulated in [7]. Hence, both benzene and triazole rings are affected on $S_1 \leftarrow S_0$ transition.

Vapour-phase absorption spectra of other BDFMH (benzo(*b*)furan, indole, benzo(*b*)thiophene, benzoxazole, benzimidazole and benzothiazole) show a very strong single $S_1 \leftarrow S_0$ origin and no long progressions [6, 7]. For benzotriazole the progression of 1 410 cm^{-1} mode, which dominates in DF spectra, does not appear in ES because of the termination of ES above 1 170 cm^{-1} from $S_1 \leftarrow S_0$ origin due to nonradiative processes.

REFERENCES

1. Nibu, Y., Abe, H., Mikami, N., Ito, M. J. Phys. Chem., 1983, **87**, 20, 3898—3901.
2. Philips, L. A., Levy, D. H. J. Chem. Phys., 1986, **85**, 3, 1327—1332.
3. Bickel, G. A., Leach, G. W., Demmer, D. R., Hager, J. W., Wallace, S. C. J. Chem. Phys., 1988, **88**, 1, 1—8.
4. Hager, J. W., Demmer, D. R., Wallace, S. C. J. Phys. Chem., 1987, **91**, 6, 1375—1382.
5. Connell, L. E., Corcoran, T. C., Joireman, P. W., Felker, P. M. Chem. Phys. Lett., 1990, **166**, 5—6, 510—516.
6. Sammeth, D. M., Yan, S., Spangler, L. H., Callis, P. R. J. Phys. Chem., 1990, **94**, 19, 7340—7342; Hollas, J. M. Spectrochim. Acta, 1963, **19**, 753—767.
7. Gordon, R. D., Yang, R. F. Can. J. Chem., 1970, **48**, 11, 1722—1729.
8. Gordon, R. D., Yang, R. F. J. Mol. Spec., 1971, **39**, 2, 295—320.
9. Rubim, J., Gutz, I. G. R., Sala, O., Orville-Thomas, W. J. J. Mol. Struct., 1983, **100**, 571—583.
10. Schütt, H.-U., Zimmermann, H. Ber. Bunsenges. Phys. Chem., 1963, **67**, 1, 54—62.
11. Escande, A., Lapasset, J., Faure, R., Vincent E. J., Elguero, J. Tetrahedron, 1974, **30**, 16, 2903—2909.
12. Escande, A., Galigne, J. L., Lapasset, J. Acta Crystallogr. B (Denmark), 1974, **B30**, Pt. 6, 1490—1495.
13. Cox, J. R., Woodcock, S., Hillier, I. H., Vincent, M. A. J. Phys. Chem., 1990, **94**, 14, 5499—5501.
14. Syage, J. A., Felker, P. M., Zewail, A. H. J. Chem. Phys., 1984, **81**, 11, 4685—4723.
15. Медведев Э. С., Ошеров В. И. Теория безызлучательных переходов в многоатомных молекулах. Москва, Наука, 1983.

Received
March 7, 1991

JOAS JAHUTATUD BENSOTRIASOOLI SPEKTROSKOOPILINE UURIMINE

On registreeritud ühelikliirusega joas jahutatud bensotriasooli molekulide laser-indutseeritud fluorestsentsi $S_1 \leftarrow S_0$ ülemineku ergastusspekter (0—0-joon sagedusel $34\,929\text{ cm}^{-1}$) ja tugevate vibronsete joonte ergastamisel saadud fluorestsentsispektrid. Erinevate vibronjoonte pöörlemiskontuuride kaju erineb oluliselt. Fluorestsentsispektrite jämeda struktuuri määrab S_0 oleku $1\,410\text{ cm}^{-1}$ võnkumise (triasooli osa asümmeetrilise venituse) pikk progressioon (kuni $\nu=6$). Oletatakse, et S_0 - ja S_1 -olekutele vastavad bensotriasooli eri tautomeerid.

Эрко ЯЛВИСТЕ, Алексей ТРЕЩАЛОВ

СПЕКТРОСКОПИЧЕСКОЕ ИССЛЕДОВАНИЕ ОХЛАЖДЕННОГО В СТРУЕ БЕНЗОТРИАЗОЛА

Измерены спектр возбуждения лазерно-индуцированной флуоресценции $S_1 \leftarrow S_0$ -перехода (0—0-линия на частоте $34\,929\text{ cm}^{-1}$) и спектр флуоресценции при возбуждении в интенсивные вибронные линии охлажденных в сверхзвуковой струе молекул бензотриазола. Форма вращательных контуров разных вибронных линий существенно различается. Грубую структуру спектров флуоресценции определяет длинная прогрессия (до $\nu=6$) колебания $1\,410\text{ cm}^{-1}$ в S_0 (асимметричное растяжение триазольной части). Предполагается, что S_0 - и S_1 -состояниям соответствуют разные таутомеры бензотриазола.

1. J. J. Van Wazer, *J. Am. Chem. Soc.*, **77**, 5715 (1955).
 2. J. J. Van Wazer, *J. Am. Chem. Soc.*, **78**, 5715 (1956).
 3. J. J. Van Wazer, *J. Am. Chem. Soc.*, **79**, 5715 (1957).
 4. J. J. Van Wazer, *J. Am. Chem. Soc.*, **80**, 5715 (1958).
 5. J. J. Van Wazer, *J. Am. Chem. Soc.*, **81**, 5715 (1959).
 6. J. J. Van Wazer, *J. Am. Chem. Soc.*, **82**, 5715 (1960).
 7. J. J. Van Wazer, *J. Am. Chem. Soc.*, **83**, 5715 (1961).
 8. J. J. Van Wazer, *J. Am. Chem. Soc.*, **84**, 5715 (1962).
 9. J. J. Van Wazer, *J. Am. Chem. Soc.*, **85**, 5715 (1963).
 10. J. J. Van Wazer, *J. Am. Chem. Soc.*, **86**, 5715 (1964).
 11. J. J. Van Wazer, *J. Am. Chem. Soc.*, **87**, 5715 (1965).
 12. J. J. Van Wazer, *J. Am. Chem. Soc.*, **88**, 5715 (1966).
 13. J. J. Van Wazer, *J. Am. Chem. Soc.*, **89**, 5715 (1967).
 14. J. J. Van Wazer, *J. Am. Chem. Soc.*, **90**, 5715 (1968).
 15. J. J. Van Wazer, *J. Am. Chem. Soc.*, **91**, 5715 (1969).
 16. J. J. Van Wazer, *J. Am. Chem. Soc.*, **92**, 5715 (1970).
 17. J. J. Van Wazer, *J. Am. Chem. Soc.*, **93**, 5715 (1971).
 18. J. J. Van Wazer, *J. Am. Chem. Soc.*, **94**, 5715 (1972).
 19. J. J. Van Wazer, *J. Am. Chem. Soc.*, **95**, 5715 (1973).
 20. J. J. Van Wazer, *J. Am. Chem. Soc.*, **96**, 5715 (1974).
 21. J. J. Van Wazer, *J. Am. Chem. Soc.*, **97**, 5715 (1975).
 22. J. J. Van Wazer, *J. Am. Chem. Soc.*, **98**, 5715 (1976).
 23. J. J. Van Wazer, *J. Am. Chem. Soc.*, **99**, 5715 (1977).
 24. J. J. Van Wazer, *J. Am. Chem. Soc.*, **100**, 5715 (1978).
 25. J. J. Van Wazer, *J. Am. Chem. Soc.*, **101**, 5715 (1979).
 26. J. J. Van Wazer, *J. Am. Chem. Soc.*, **102**, 5715 (1980).
 27. J. J. Van Wazer, *J. Am. Chem. Soc.*, **103**, 5715 (1981).
 28. J. J. Van Wazer, *J. Am. Chem. Soc.*, **104**, 5715 (1982).
 29. J. J. Van Wazer, *J. Am. Chem. Soc.*, **105**, 5715 (1983).
 30. J. J. Van Wazer, *J. Am. Chem. Soc.*, **106**, 5715 (1984).
 31. J. J. Van Wazer, *J. Am. Chem. Soc.*, **107**, 5715 (1985).
 32. J. J. Van Wazer, *J. Am. Chem. Soc.*, **108**, 5715 (1986).
 33. J. J. Van Wazer, *J. Am. Chem. Soc.*, **109**, 5715 (1987).
 34. J. J. Van Wazer, *J. Am. Chem. Soc.*, **110**, 5715 (1988).
 35. J. J. Van Wazer, *J. Am. Chem. Soc.*, **111**, 5715 (1989).
 36. J. J. Van Wazer, *J. Am. Chem. Soc.*, **112**, 5715 (1990).
 37. J. J. Van Wazer, *J. Am. Chem. Soc.*, **113**, 5715 (1991).
 38. J. J. Van Wazer, *J. Am. Chem. Soc.*, **114**, 5715 (1992).
 39. J. J. Van Wazer, *J. Am. Chem. Soc.*, **115**, 5715 (1993).
 40. J. J. Van Wazer, *J. Am. Chem. Soc.*, **116**, 5715 (1994).
 41. J. J. Van Wazer, *J. Am. Chem. Soc.*, **117**, 5715 (1995).
 42. J. J. Van Wazer, *J. Am. Chem. Soc.*, **118**, 5715 (1996).
 43. J. J. Van Wazer, *J. Am. Chem. Soc.*, **119**, 5715 (1997).
 44. J. J. Van Wazer, *J. Am. Chem. Soc.*, **120**, 5715 (1998).
 45. J. J. Van Wazer, *J. Am. Chem. Soc.*, **121**, 5715 (1999).
 46. J. J. Van Wazer, *J. Am. Chem. Soc.*, **122**, 5715 (2000).
 47. J. J. Van Wazer, *J. Am. Chem. Soc.*, **123**, 5715 (2001).
 48. J. J. Van Wazer, *J. Am. Chem. Soc.*, **124**, 5715 (2002).
 49. J. J. Van Wazer, *J. Am. Chem. Soc.*, **125**, 5715 (2003).
 50. J. J. Van Wazer, *J. Am. Chem. Soc.*, **126**, 5715 (2004).
 51. J. J. Van Wazer, *J. Am. Chem. Soc.*, **127**, 5715 (2005).
 52. J. J. Van Wazer, *J. Am. Chem. Soc.*, **128**, 5715 (2006).
 53. J. J. Van Wazer, *J. Am. Chem. Soc.*, **129**, 5715 (2007).
 54. J. J. Van Wazer, *J. Am. Chem. Soc.*, **130**, 5715 (2008).
 55. J. J. Van Wazer, *J. Am. Chem. Soc.*, **131**, 5715 (2009).
 56. J. J. Van Wazer, *J. Am. Chem. Soc.*, **132**, 5715 (2010).
 57. J. J. Van Wazer, *J. Am. Chem. Soc.*, **133**, 5715 (2011).
 58. J. J. Van Wazer, *J. Am. Chem. Soc.*, **134**, 5715 (2012).
 59. J. J. Van Wazer, *J. Am. Chem. Soc.*, **135**, 5715 (2013).
 60. J. J. Van Wazer, *J. Am. Chem. Soc.*, **136**, 5715 (2014).
 61. J. J. Van Wazer, *J. Am. Chem. Soc.*, **137**, 5715 (2015).
 62. J. J. Van Wazer, *J. Am. Chem. Soc.*, **138**, 5715 (2016).
 63. J. J. Van Wazer, *J. Am. Chem. Soc.*, **139**, 5715 (2017).
 64. J. J. Van Wazer, *J. Am. Chem. Soc.*, **140**, 5715 (2018).
 65. J. J. Van Wazer, *J. Am. Chem. Soc.*, **141**, 5715 (2019).
 66. J. J. Van Wazer, *J. Am. Chem. Soc.*, **142**, 5715 (2020).
 67. J. J. Van Wazer, *J. Am. Chem. Soc.*, **143**, 5715 (2021).
 68. J. J. Van Wazer, *J. Am. Chem. Soc.*, **144**, 5715 (2022).
 69. J. J. Van Wazer, *J. Am. Chem. Soc.*, **145**, 5715 (2023).
 70. J. J. Van Wazer, *J. Am. Chem. Soc.*, **146**, 5715 (2024).
 71. J. J. Van Wazer, *J. Am. Chem. Soc.*, **147**, 5715 (2025).